Molecular Dynamics Investigation of the Transient Regime in the Freezing of Salt Clusters

Yuriy G. Bushuev[†] and Lawrence S. Bartell*

Department of Chemistry, University of Michigan, Ann Arbor, Michigan 48109

Received: September 5, 2006

Molecular dynamics (MD) investigations of the freezing of supercooled liquids can identify nuclei far smaller than can be detected in laboratory experiments, to date, and consequently can provide information about nucleation so far inaccessible to experiment. In a recent MD study of the freezing of clusters of SeF_6, a new method of recording nucleation events was introduced. It involved the observation of times of first appearance of nuclei of the size of *n*. An advantage of the new approach is that it provides information about the size of the critical nucleus. For nuclei smaller than the critical size, it also avoids the overshoots of nucleation rates that precluded the application of the Miloshev−Wu method in the subcritical region. Kinetic information in the transient regime can be characterized by three parameters, the time lag, the reduced moment, and the steady state nucleation rate. To get some idea of how general the new approach is, a very different system was investigated, that of clusters of NaCl. Two different fitting functions were used to analyze the results. The first one adopted the log-normal probability distribution of Wu. The second function was a modification of Shneidman's analytical solution appropriate for large nuclei. The second function gave a rather good account of MD data for all nuclear sizes and temperatures and gave more stable results in the subcritical region. Several inferences of the sizes of critical nuclei were made. Applying the criterion for n^* based on the Zeldovich solution of the Becker−Döring equations, we estimated the critical nucleus sizes to be 14, 18, and 24 ions for quench temperatures of 640, 690, and 740 K, respectively. Even though the interionic interactions initiating nucleation in salt are very different from the van der Waals interactions in clusters of SeF_6, the characteristic aspects of the transient regimes of the two systems were quite similar.

Introduction

Phase transformations are important in science and technology. They are normally initiated by nucleation. The phase generated may depend upon the conditions of nucleation. A more complete understanding of such matters as nucleation in cloud formation or in the control over phases nucleated in industrial processes would be valuable. While academic studies of nucleation have concentrated on homogeneous nucleation, the most common type of nucleation encountered in technology is heterogeneous. Nevertheless, the theory of heterogeneous nucleation is based on the framework of homogeneous nucleation, and this theory is incomplete. The nucleation theory that has been most thoroughly studied concerns the condensation of vapor to liquid. In the present investigation, we treat the pseudohomogeneous nucleation[1] in freezing, a process for which nucleation theory is at an earlier stage of development. By pseudohomogeneous nucleation (sometimes referred to as homogeneous surface nucleation), we mean that nucleation takes place in perfectly pure, uncontaminated clusters in our system but tends to occur preferentially at cluster surfaces rather than uniformly throughout the volume of the clusters. Therefore, surfaces appear to catalyze nucleation. Computer experiments in the form of molecular dynamics (MD) simulations of clusters provide the data to be analyzed.

An important consideration in theory is the behavior of $J(n,t)$, the time development of the nucleation rate as a function of the size, *n*, of a nucleus formed. In particular, we are concerned with the transient regime, the time before a steady state has been attained. It was Turnbull[2,3] who first developed experimental techniques to study homogeneous nucleation in freezing, as well as a theoretical framework to account for experimental observations. He found ways to subdivide supercooled liquid systems into well-characterized droplets so small that most individual droplets could be expected to be free from contaminants that might lead to heterogeneous nucleation. Besides being a difficult, demanding technique, his method was incapable of studying nucleation in the transient regime.

One difficulty with experimental studies is that nucleation cannot be detected until the nuclei are observed, and these cannot be recognized until nuclei are enormously larger than critical nuclei. A virtue of MD simulations is that solid nuclei can be identified in a large mass of liquid even when the nuclei are smaller than n^*, the critical size. A prime quantity sought in conventional nucleation studies is $N(n,t)$, the number of nuclei per unit volume of size *n* or greater attained at time *t*. Observations of this quantity do not lend themselves to the inference of n^*, the size of the critical nucleus. Although the behavior of $N(n,t)$ in the transient regime depends on *n*, the steady state rate, given by the slope at large time, is independent of *n*. It was recently shown[4] that if times of first appearance of nuclei of size *n* are determined instead of $N(n,t)$, the results contain information about n^*.

Therefore, the main thrust of this work is related to the determination of times of first appearance of nuclei of size *n* in MD simulations. The first publication[4] to use times of first appearance was based on a system of molecular clusters of the compound SeF_6. To what extent its findings revealed generalities

* Corresponding author. E-mail: lbart@umich.edu.

[†] Permanent address: Ivanovo State University of Chemistry and Technology, Engelsa, 7, Ivanovo, Russia. E-mail: bushuev@isuct.ru;yuriyb2005@gmail.com.

10.1021/jp068086r CCC: $37.00
Published on Web 01/31/2007

could only be determined by further studies of different systems. Therefore, instead of using a system of quasi-spherical polyatomic molecules bound by van der Waals forces, we adopt the very different system of NaCl, whose ions are bound primarily by electrostatic forces. Although several MD studies of the freezing of molten salt clusters have been reported,[5−7] none so far have recorded enough nucleation events to characterize the transient regime.

Miloshev's probabilistic approach[8] is based on a formal coincidence of the expression for time lag, the value adopted in transport theories,[9] with the first moment of the cumulative probability distribution function. This approach suggested the idea of treating nucleation as a random process with an attributed probability distribution. Wu proposed[10] to express the distribution by parameters of a suitable function and established the parameters by requiring the first two moments of the function he chose, namely, a log-normal distribution, to reproduce exactly those moments of an exact numerical solution of the Becker−Döring coupled differential equations. In conventional investigations, the probabilistic approach has not been applicable to the subcritical region, because the generally applied Becker−Döring−Zeldovich theory[11,12] yields solutions[9,13,14] for reduced flux that overshoot the steady state value for $n < n^*$, giving negative, and hence unacceptable, values to the Miloshev probability distribution. Use of the method of times of first appearance avoids the overshooting and provides probabilistic information into the subcritical region.

The question about possible analytical expressions for the probability distribution is an open question. In addition to the log-normal distribution function introduced by Wu, we examine another function based on a modification of Shneidman's asymptotic analytical solution of the Becker−Döring equations.

Method

Simulations. Molecular dynamics simulations were carried out with a program designed to handle clusters of sodium chloride possessing neither translational nor rotational angular momentum. The program was based on ref 15, using the leapfrog algorithm for integrating the equations of motion with a 5 fs time step. The Born−Mayer−Huggins potential incorporating the parameters of Tosi and Fumi[16] was adopted. Simulations were performed in two stages.

In the first stage were prepared 4000 independent initial configurations of molten NaCl clusters containing 500 cations and 500 anions. This was done by constructing a face-centered cubic cluster of salt with 1000 ions and melting it thoroughly. After melting, it was equilibrated to 900 K using simple velocity rescaling to maintain the temperature. At this temperature, cooler than the freezing point, nucleation was too slow to occur on the time scale of our computations (∼100 ns), and no evaporation occurred. After thermal and structural relaxation, configurations were collected at intervals of 10 ps to serve as independent molten clusters for simulations. Independence was inferred from the absence of any correlation between nucleation times and order of collection.

In the second stage, the 4000 clusters were quenched to predetermined temperatures, which were maintained using the Nosé−Hoover thermostat with the adjustable parameter τ_T set to 0.1 ps.

Identification of Solid Nuclei in Molten Clusters. In any investigation of nucleation, it is necessary to recognize small nuclei in the presence of a large amount of the mother phase. In condensation, this is far simpler than in the case of freezing, of course, and results for freezing depend upon the particular order parameter selected to identify the embryos or nuclei involved. Voronoi polyhedra can provide an exquisitely sensitive method for the interior of clusters but one not suited to handle surface molecules. In view of the fact that surface nucleation is probable, the Voronoi method is less suitable for clusters (with a high surface-to-volume ratio) than some other methods. In the present study, we adopted the bond-order parameter method[17,18] to analyze molecular environments because it allows us to take surface molecules into consideration, as well. The "Q_6" method was found to be quite appropriate in investigations[19] of clusters of SeF_6. In the case of a system of identical atoms or molecules, Frenkel et al.[17,18] introduced the matrix elements

$$\bar{q}_{lm}(i) = \frac{1}{N_b(i)} \sum_{j=1}^{N_b(i)} Y_{lm}(\hat{\mathbf{r}}_{ij}) \tag{1}$$

where $N_b(i)$ is the number of particles surrounding particle i, $\hat{\mathbf{r}}_{ij}$ is a unit vector connecting particles i and j, and the Y_{lm} are the spherical harmonics. To construct a rotationally invariant scheme, they attributed a 13-dimensional unit vector, $\mathbf{q}_6(i)$, to every particle, with components

$$\tilde{q}_{6m}(i) = \frac{\bar{q}_{6m}(i)}{\left[\sum_{m=-6}^{6} |\bar{q}_{6m}(i)|^2\right]^{1/2}} \tag{2}$$

The dot product $\mathbf{q}_6 \cdot \mathbf{q}_6$ gives the desired invariant. To identify solidlike particles, they introduced two adjustable parameters. In the case of an atomic system, Frenkel et al. defined atom i to be "solidlike" if it was surrounded by seven atoms whose dot product with i exceeded 0.5. In a treatment of clusters of SeF_6, the same criterion considering the central selenium atom to be i was used.[19] In the case of surface molecules, which have fewer neighbors, we relaxed the number required for i to belong to a solidlike molecule.

For clusters of salt, Frenkel's method was implemented as follows. We identified the "bonds" between ions of like charge if the dot product $\mathbf{q}_6 \cdot \mathbf{q}_6$ exceeded 0.6 and the ions were no further apart than 4.5 Å. Such a value is plausible in view of the fact that the closest distance between ions of like charge in the NaCl crystal is 3.98 Å. However, in studying nucleation, it is not enough to identify solidlike ions. Because of random structural fluctuations at deep supercooling, it has been found that so many ions qualifying as solidlike pop into existence that the noisy plots of their number give no clear indication of the true onset of nucleation. Many potentially pertinent solidlike embryos whose size would seem to be large enough to qualify as nuclei are thin sheets or filaments whose presence does not correlate well with nucleation. It has been found to be more productive in diagnoses of nucleation to consider "bulklike" ions which are solidlike but also belong to specific elements of the salt crystalline structure. If ions of a given charge are considered, it can be seen that the main structural elements of the NaCl sublattice are tetrahedra and semi-octahedra. We used these structural motifs in our search for bulklike ions. We define nuclei as bulklike if they contain tetrahedra or semi-octahedra. When these bulklike nuclei are considered, times of first appearance of n-mers exhibit the behavior found in an earlier study[4] of the freezing of clusters of SeF_6 and can be analyzed in terms of the three parameters of the Miloshev−Wu method,[8,10] namely, the steady state rate, J_s, the time lag, L, and the reduced moment, M_r, a quantity to be defined in the following.

Although prior studies of salt encountered problems with edge and corner ions, we had no such trouble with those ions when we applied our criteria. The occurrence of multiple nuclei did become somewhat troublesome. Often several nuclei formed at almost the same time (all appearing within the same finite time step) when molten clusters were highly supercooled. Some of them disappeared quickly. Because the orientations of the principal axes of the crystalline nuclei were random, as a rule, they did not appear as a consequence of a failure to completely melt the solid when liquid clusters were generated. In any event, our analyses are based on the times of first appearance of nuclei of size n. When several bulklike nuclei materialized in the same time step, t_i, we selected the largest of them for the time of first appearance of a nucleus of that size. In the case of multiple nuclei, we identified the largest nucleus, namely, an assembly of contiguous ions, using a method of analysis based on the connectivity matrix introduced by Sevick et al.[20] To be included in that nucleus, a bulklike ion was required to be within 4 Å of the closest of the other members.

Analysis of Molecular Dynamics Simulations. Sets of molecular configurations for every cluster were obtained in the molecular dynamics simulations. We calculated the size of nuclei for every configuration and determined the times of first appearance of n-ion nuclei. After that, we considered the cluster as nucleated and discarded it from further consideration pertaining to n-mers. The fraction of nucleated clusters, $F(n,t)$, at time t is an observable of the MD simulation. Kinetic curves of $F(n,t)$ contain all the information about the nucleation process. Our approach has some simplification. We consider the net rate of production of n-mers from precursor nuclei. This corresponds to the solution of the kinetic equation[2,10] for the transient nucleation stage

$$J(n,t) = \beta_{n-1} f_{n-1}(t) - \alpha_n f_n(t) \tag{3}$$

with specific boundary conditions

$$f_1(t) = \text{const}, \quad f_m(t) = 0$$

Here, β_{n-1} denotes the attachment rate of monomers to a nucleus of size $n-1$, α_n denotes the detachment rate from the nucleus, and $f_n(t)$ is the number of n-mers per unit volume. Usually, the governing equation is solved taking $m \gg n^*$. Because we remove clusters after nucleation and consider only cluster statistics,[19] the determined nucleation rate for times of first appearance differs from the true net nuclear grown rate. When we encountered multiple nucleation events in cluster volumes at the same time step, we took into consideration only the largest nucleus. These simplifications were important mainly for subcritical nuclei. Of particular importance is the reduced flux, $\phi(n,t) = J(n,t)/J_s$, the ratio of the nucleation rate at time t to the steady state rate of nucleation. This function plays a significant role in most theories of nucleation and is related to $F(n,t)$ as follows.

As was shown in previous papers,[4,19]

$$F(n,t) = 1 - \exp[-KS(n,t)] \tag{4}$$

where K is the product $J_s V_c$, with V_c corresponding to the cluster volume, and

$$S(n,t) = \int_0^t \phi(n,t')\, dt' \tag{5}$$

In principle, it is possible to calculate the reduced flux, $\phi(n,t)$, using numerical differentiation methods. However, commonly speaking, this is an ill-posed mathematical problem[21] and the task has no unique solution. Significantly different solutions reproduce observable values to within statistical error.

Several theoretical approaches to the nucleation problem give analytical expressions for the reduced flux. One of the approaches is based on the theory of probabilities. Miloshev[8] noted that in some cases the reduced flux can be treated as a consequence of a cumulative probability distribution function. A probability distribution function, ρ, is associated with $\phi(t)$ by the relation $\rho(t) = \partial\phi(t)/\partial t$. Wu showed[10] numerically that for large nuclei ($n \gg n^*$) the familiar log-normal distribution approximated exact numerical Becker−Döring solutions[14] very well. The log-normal distribution has two parameters, a and b.

$$\rho(x) = \frac{\exp[-(\ln x - a)^2/2b^2]}{x\sqrt{2\pi b^2}} \tag{6}$$

One problem is that the probabilistic approach is not applicable for $n < n^*$ in conventional analyses of data where overshooting of $J(t)$ over the steady state value, J_s, has been demonstrated numerically[13] and analytically.[22] As mentioned above, this leads to negative probability distributions. However, if we determine, instead, the times of first appearance, the probabilistic interpretation appears to be satisfactory for our task for all n.

If the probabilistic approach allows a speculative exploration and can be based on additional assumptions and empirical data, the equation for reduced flux obtained by Shneidman[23,24] may be useful. Shneidman's function, the extreme value Gumbel distribution,[25] is an analytical solution of the classical nucleation problem appropriate for large nuclei. It is expressed as the double exponential function

$$\phi^{\mathrm{Sh}}(n,t) = \exp\left[-\exp\left(\frac{t_i(n) - t}{\tau}\right)\right] \tag{7}$$

where the function $t_i(n)$ is the incubation time and the constant τ is the relaxation time. For large n, $\phi(n,t)$ satisfies the demands for cumulative probability. It means that the adjustable parameters of eq 7 may be expressed through the statistical moments.

$$M_k(n) = \int_0^\infty t^k [1 - \phi(n,t)]\, dt = \frac{1}{k+1}\int_0^\infty t^{k+1} \rho(n,t)\, dt \tag{8}$$

The 0th moment is the time lag, L, the parameter widely used in nucleation theory. A simple reduced flux formula may be written using the reduced moment, $M_r = 2M_1/M_0^2$. It was shown that, for Wu's expression,

$$\phi^{\mathrm{Wu}}(\Theta) = 1 - \frac{1}{2}\,\mathrm{erfc}\left[\frac{\ln(\Theta\sqrt{M_r})}{\sqrt{2\ln M_r}}\right] \tag{9}$$

and, for Shneidman's,[23]

$$\phi^{\mathrm{Sh}}(\Theta) = \exp\left[-\exp\left(-\frac{\pi}{\sqrt{6}}\frac{\Theta - 1}{\sqrt{M_r - 1}} - \gamma\right)\right] \tag{10}$$

where $\Theta = t/L$ is the reduced time and $\gamma = 0.5772...$ is Euler's constant.

We cannot directly use the Shneidman function as a cumulative distribution for all parameters, because the cumulative probability function, $\phi(t)$, must start from zero and increase monotonically to unity. For function 10, the first condition is not satisfied. If M_r is close to 1, the difference between $\phi^{\mathrm{Sh}}(0)$

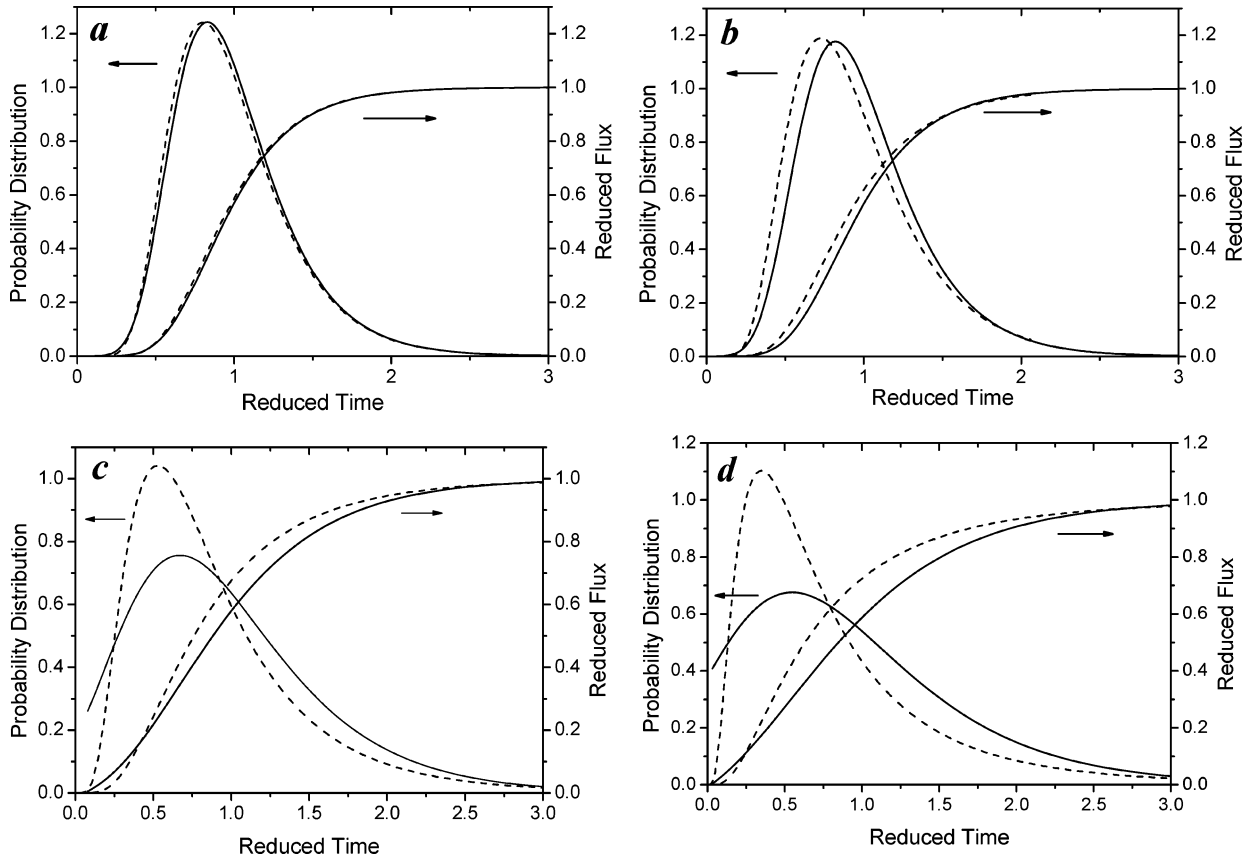

Figure 1. Probability distribution function and reduced flux for $n = 150$ ions, or 75 NaCl pairs: (a) $T = 740$ K; (b) $T = 640$ K. For $n = 18$, (c) $T = 740$ K and (d) $T = 640$ K. Solid curves, according to eq 11; dashed curves, according to eq 6.

and zero is very small. However, for $M_r = 2$, a value not infrequently encountered, $\phi^{Sh}(0)$ is 0.132, a value too far from zero to be acceptable. In order to obtain a trial function of possible utility, we therefore modified the Shneidman function as follows, in such a way that the demands of the probabilistic method are fulfilled. First, we constructed the probability density function as a derivative of ϕ^{Sh} and took into consideration the normalization demand

$$\rho^{trial}(t) = C \exp\left[-\exp\left(-\frac{\pi}{\sqrt{6}}\frac{t-\vartheta}{\vartheta\sqrt{q-1}} - \gamma\right)\right] \left[-\exp\left(-\frac{\pi}{\sqrt{6}}\frac{t-\vartheta}{\vartheta\sqrt{q-1}} - \gamma\right)\right]\left(-\frac{\pi}{\sqrt{6}}\frac{1}{\vartheta\sqrt{q-1}}\right)$$

$$C = 1/\int_{t_1}^{t_2}\rho^{trial}(t)\,dt \qquad (11)$$

where ϑ and q are adjustable parameters, C is a normalization constant, and t_1 and t_2 are the starting and finishing times of the crystallization process. We assumed $t_1 = 0$ and $t_2 = \infty$. According to these conditions,

$$\phi^{trial}(t) = \int_0^t \rho^{trial}(x)\,dx = \frac{\phi^{Sh}(t) - \phi^{Sh}(0)}{1 - \phi^{Sh}(0)} \qquad (12)$$

The new function ϕ^{trial}, which coincides with ϕ^{Sh} as $q \rightarrow 1$, does not yield a trial density function, $\rho^{trial}(t)$, that vanishes at $t = 0$ nor does it have $n - 2$ derivatives of zero at $t = 0$, as would a function[23] that corresponded to a solution of the Becker−Döring coupled differential equations of classical theory. Nevertheless, we adopt it as a trial function to see how it works. We note that the log-normal distribution, as well, also has an asymptotic behavior at $t \rightarrow 0$ that is not in accord with Becker−Döring solutions. We used eq 8 for calculation of the moments of the trial distribution function.

For a given proposed expression for $\phi(n,t)$, the standard way of defining the best fit with the simulation data is to refine the three parameters that minimize the sum of the squares of the deviation of a theoretical curve, $F(t)$, calculated by eq 4 from the experimental points, y_i, or

$$\chi^2(K,d,e) = \frac{1}{m-3}\sum_{i=1}^{m}[y_i - F(t_i,K,d,e)]^2 \qquad (13)$$

where $d = L$ and $e = M_r$ for the log-normal distribution and $d = \vartheta$ and $e = q$ for eq 11. Typically, least-squares fits involving multiple parameters can lead to multiple minima. To find the global minimum, we calculated values of χ^2 on a grid, (K_i,d_j,e_k), and the lowest value was taken to correspond to the desired set of parameters.

Results

Nucleation occurring in sets of molten salt clusters was studied at quench temperatures of 740, 690, and 640 K. Analyses were carried out using both eqs 6 and 11. Application to MD data of the two functions for large nuclei, say at $n = 150$ ($n \gg n^*$), gave very similar results for the probability distribution and reduced flux functions, as is shown in Figure 1a and b. However, the differences between the curves increase markedly when n drops to 18 ($n \approx n^*$). The discrepancies get larger at deeper supercooling, where the barrier to nucleation is lower (Figure 1c and d). Reduced flux and probability distribution functions are associated with the first and second derivatives of the experimental MD data.

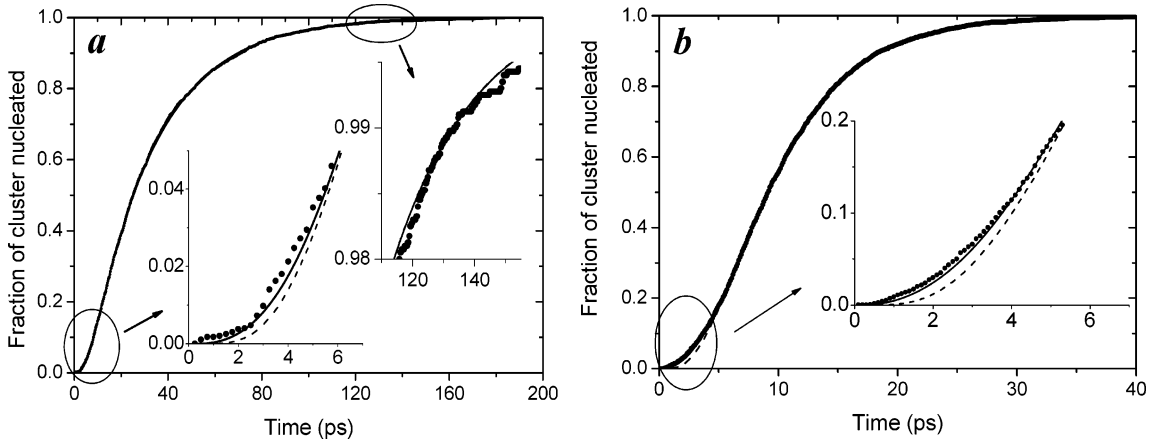

Figure 2. Time evolution of fractions of clusters that have generated nuclei of (a) $n = 18$ ions at $T = 740$ K and (b) $n = 16$ ions at $T = 690$ K: points, MD data; solid curves, least-squares fitting according to eq 11; dashed curves, fitting according to eq 6.

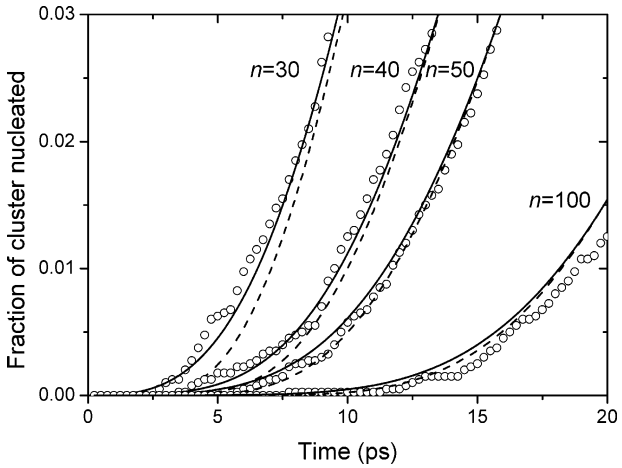

Figure 3. Time evolution of fractions of clusters that have generated n nuclei after quench at 740 K: points, MD data; solid curves, least-squares fitting according to eq 11; dashed curves, fitting according to eq 6.

Figures 2−4 illustrate the quality of fitting of MD data as it depends on nuclear size and stage of nucleation. Both functions yield excellent approximations at long t for most values of n. The more problematic region is at small time. In curves presented in Figures 3 and 4, fewer than 10% of the clusters have experienced nucleation. It is to be noted that the discrepancies between the two different schemes of analysis in these examples are only of the order of 10^{-3}. Our trial function eq 11 gives better results in the near critical region, especially at the first stage of nucleation. In Figure 4b, the reverse is true. For small nuclei, the log-normal function failed to give stable results, and sometimes, its application eluded reasonable solutions. The applicability of eq 6 to $n < n^*$ regions seems problematic.

Curious isosbestic points in Figure 5 are encountered in curves of the probability distributions and reduced fluxes versus reduced time as n increases, when refinements are based on eq 11. Reduced flux curves intersect at $\Theta = 1$ for large n and at $\Theta = 1.2$ for small n. This behavior implies two regimes of nucleation in sub- and supercritical regions, at least in analyses based on times of first appearance. There are two intersections of probability distribution curves, ρ^{trial}, at 0.6 and 1.4 for $n > n^*$ and at 0.45 and 1.8 for $n < n^*$. Figure 6 also shows that fitting curves suggest the existence of two nucleation regimes. Smaller embryos are formed at smaller reduced times. The situation is drastically changed for larger nuclei. $F(n,t)$ curves intersect at short time ($\Theta = 0.75$), and after that, smaller nuclei are formed at longer reduced times. The reason for such behavior lies in the dependence of time lag on nuclear size.

Figure 7 shows that the two methods of fitting MD data gave slightly different time lags for the same nuclear sizes, and the differences increase with decreasing temperature. Other dependences of adjustable parameters versus nuclear size are presented in Figure 8. The nucleation rates and reduced moments determined using eqs 6 and 11 are close to each other, especially at 740 K. The log-normal distribution gave unstable results at 640 K for small n. High values of mutual correlation coefficients of parameters interfere with accuracy. The function χ^2 has many

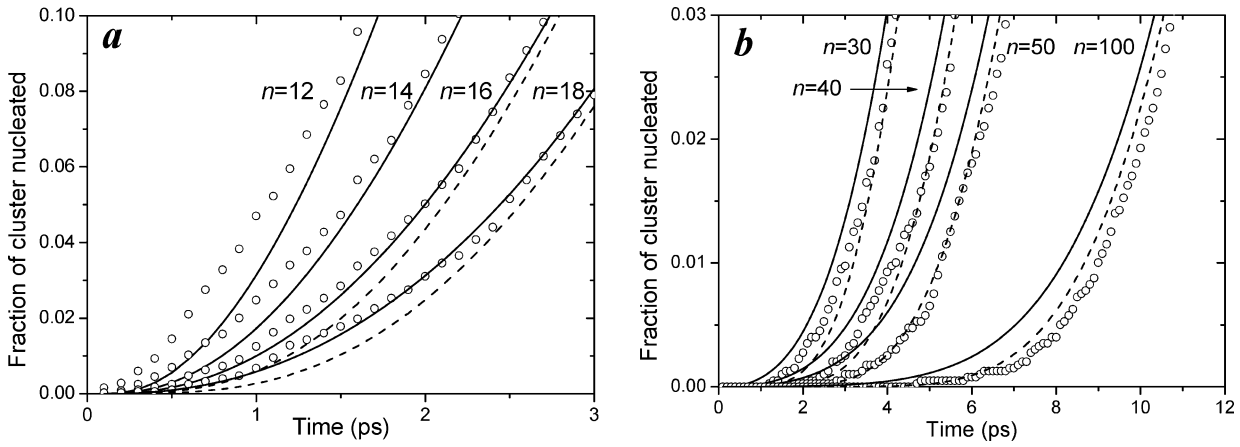

Figure 4. Same as Figure 9 but for 640 K.

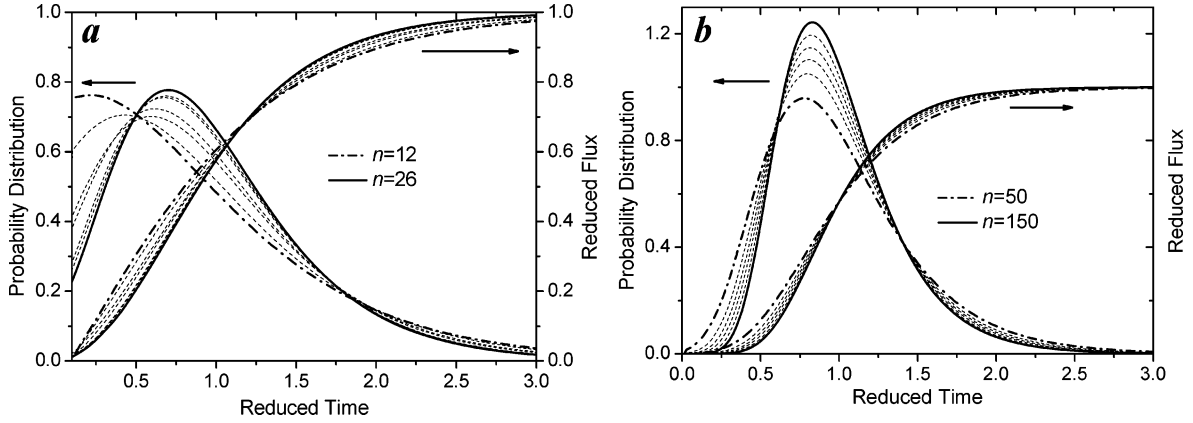

Figure 5. Probability distribution (eq 11) and reduced flux functions at $T = 740$ K for subcritical (a) and supercritical nuclei (b). The dot−dashed curves are for the smallest n, the solid curves are for the largest n, and the dashed curves are for intermediate n values.

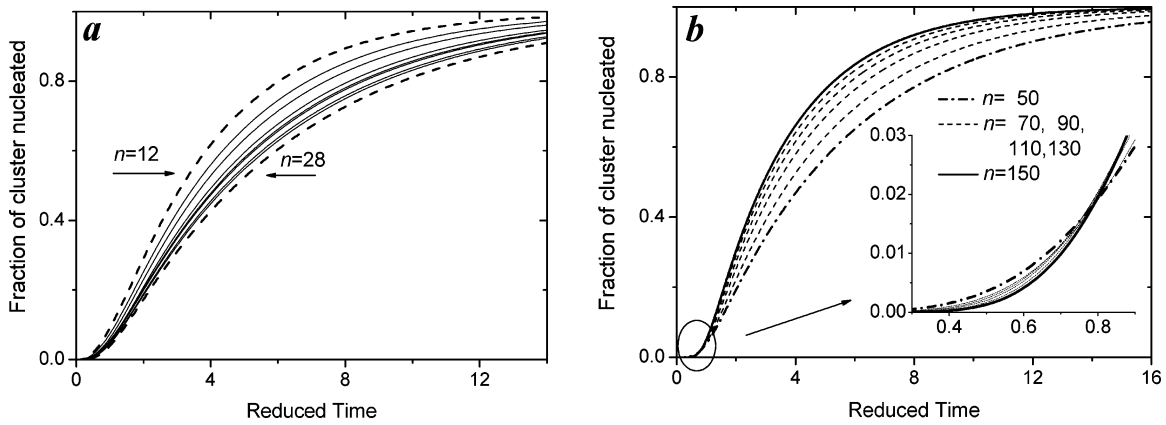

Figure 6. Fractions of clusters that have generated n nuclei at 740 K for (a) subcritical and (b) supercritical nuclei vs reduced time t/L.

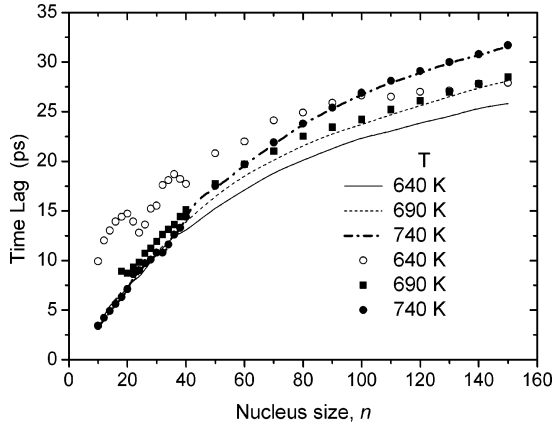

Figure 7. Time lag vs nuclear size: curves, according to eq 11; circles, according to eq 6.

local minima. Different triplets (K, L, M_r) give approximately the same quality of fitting the MD data.

Discussion

Simulations of the process of freezing of salt clusters were consistent in many aspects with those of prior simulations published[4,19] by this laboratory, but because the present simulations included enormously larger sets of nucleation events, they revealed much more detail about the process, particularly in the transient regime. Results are also broadly consistent with those published by Valariani et al.,[7] who studied nucleation rates of salt clusters at much higher temperatures but did not examine the transient regime. At the rather deep quenches of the present computations, nearly simultaneous multiple nucleation events in individual clusters occurred that somewhat complicated analyses of nucleation parameters.

Derivations of the nucleation parameters, namely, the steady state rate of nucleation, K, the time lag, L, and the reduced moment, M_r, were carried out using the two different proposed expressions. Wu's empirical expression based on a log-normal representation (eq 6) of $\rho(n,t)$ was directly applied. Shneidman's asymptotic solution of the coupled equations of Becker−Döring theory was applied in a modified version (eqs 11 and 12). It had originally been intended to apply only to high barriers, that is, for shallower degrees of supercooling and, hence, is applicable only in the case of very large nuclei. To avoid the nonzero value of the Shneidman function at zero time, a simple stratagem was put into force, that of modifying the function as shown in eq 11. When nuclei were large, the Shneidman expression could be used without transformation, and in this case, results were very close to the results obtained by the Miloshev−Wu approach.

Koishi et al.[6] simulated nucleation of NaCl at 640 and 740 K for large numbers of ions in clusters (13 824 ions), and in a cell (13 824 and 125 000 ions) with periodic boundary conditions (PBC). The associated nucleation rates, J_s, in m^{-3} s^{-1}, derived were 14.4×10^{35} at 640 K and 0.75×10^{35} at 740 K for clusters. For the unlimited systems, the rates were 6.6×10^{35} and 1.67×10^{35}, respectively. At the same temperature, the values differ approximately by a factor of 2 depending on the nucleation conditions. The application of PBC led to rate decreases at 640 K and increases at 740 K. This counterintuitive behavior may be the consequence of large uncertainties due to the small number of runs, only 38 in number. Valeriani et al.[7]

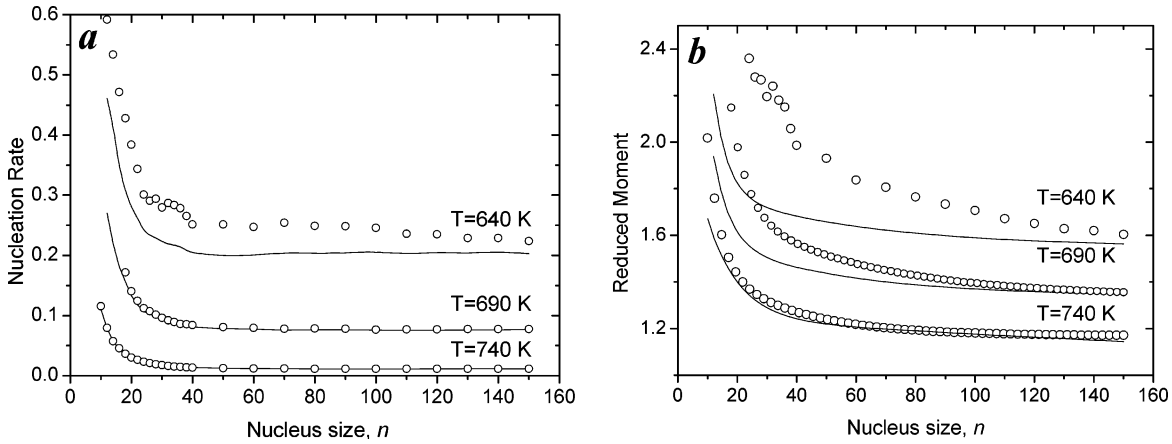

Figure 8. Dependences on nuclear size of (a) steady state nucleation rate, K (number of cluster nucleation events per picosecond), and (b) reduced moment: solid curves, least-squares fitting according to eq 11; open circles, fitting according to eq 6. Data for the reduced moment were shifted for clarity upward by 0.2 at 690 K and by 0.4 at 640 K.

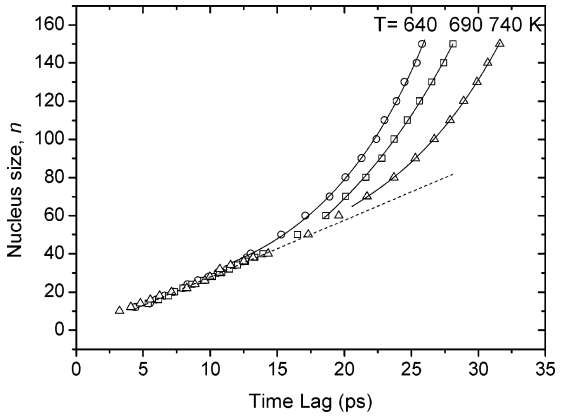

Figure 9. Nuclear size vs time lag calculated according to eq 11. The symbols are for the first stage of nucleation, the symbols and solid lines are for the second stage, and the dashed straight line is a fit of the first stage.

simulated a system of 3456 ions with PBC, and they estimated $J_s \sim 10^{35}$ at 740 K.

We calculated the steady state rate, $J_s = K/V_c$, where K was determined at $n = 150$ and V_c was calculated from the numerical density of the clusters.[6,7] Our values are 70×10^{35} (640 K), 26×10^{35} (690 K), and 3.9×10^{35} m^{-3} s^{-1} (740 K). These values are of the same order of magnitude as those found in previous studies in this laboratory but are several times larger than Koishi values. The difference is at least in the direction expected from the influence of cluster surface on nucleation, inasmuch as the surface-to-volume ratio is greater for smaller clusters. We studied what might be expressed as pseudohomogeneous nucleation, because in most cases nucleation occurred near the cluster surface.

In the literature, there are two independent estimations of critical nuclei size for NaCl. Koishi et al.[6] estimated $n^* = 120-130$ ions at 640 and 740 K. The apparent temperature independence contradicts classical theory and the results of Valeriani et al.,[7] who estimated that $n^* = 120$ at 800 K and 150 ions at 825 K. Even at first glance, our results show, in agreement with Valerian et al.,[7] that the lower the temperature, the smaller the critical nucleus. If we were to adopt the proposition[7] that $n^* \propto (1 - T/T_m)^{-3}$, where $T_m = 1060$ K is the melting temperature of NaCl in our model, we might expect $n^* = 28$, 40, and 62 at 640, 690, and 740 K, respectively. This empirical relation is not expected to be particularly accurate, but it gives the general magnitude of sizes of critical nuclei found in our own simulations. Also, as explained above, our nucleation of clusters can be considered to be heterogeneous because of the role of the surface in nucleation.

It was shown[4] that the size of the critical nucleus can be inferred from the size at which the steady state rate corresponding to times of first appearance is twice that determined for the steady state of large nuclei. This result is a consequence of the application of Zeldovich's solution to the nucleation problem. Applying this criterion for n^* to the $K(n)$ data gives values for the sizes of critical nuclei of 14, 18, and 24 ions for quench temperatures of 640, 690, and 740 K, respectively. This increase in size with increasing temperature is consistent with nucleation theory, in general, and with the results of Valerian et al.[7] An estimation of uncertainties to be expected from this treatment will be published subsequently.

In addition to the estimate of the size of the critical nucleus by applying the Zeldovich solution, there are other suggestive features in the MD data which deserve consideration. The data reveal two regimes of nucleation in plots of various observables. Clearly, for nuclei smaller than the critical size, there is a tendency for the nuclei to decay, and for nuclei larger than the critical size, there is a tendency for the nuclei to grow. It is possible that such tendencies are reflected in some of the observables. For example, the curves of nuclear size versus time lag in Figure 9 display two regions. For the first stages of nucleation, they do not depend on temperature, and all data may be fitted by one straight line. In the second stage, the curves are separated. We estimated the positions of bifurcation points for every temperature. The straight line and curves start to diverge approximately at $n = 28$ (640 K), 36 (690 K), and 48 (740 K). It is suggestive that these numbers are of the same magnitude as the values for n^* derived above. Moreover, the curves for the nucleation rate and reduced moment plotted on a logarithmic scale, as shown in Figure 10, can be approximated in each case by two straight lines. Their points of intersection are at approximately $n = 20$ (640 K), 25 (690 K), and 33 (740 K). Again, these values are of the same magnitude as those derived above for the size of the critical nucleus. All sets of values of nuclear size apparently related to the critical phenomenon, sizes as estimated by various observables, are presented in Figure 11. A theoretical investigation of possible links between the regions of distinctly different behavior and the size of the critical nucleus would be worth investigating.

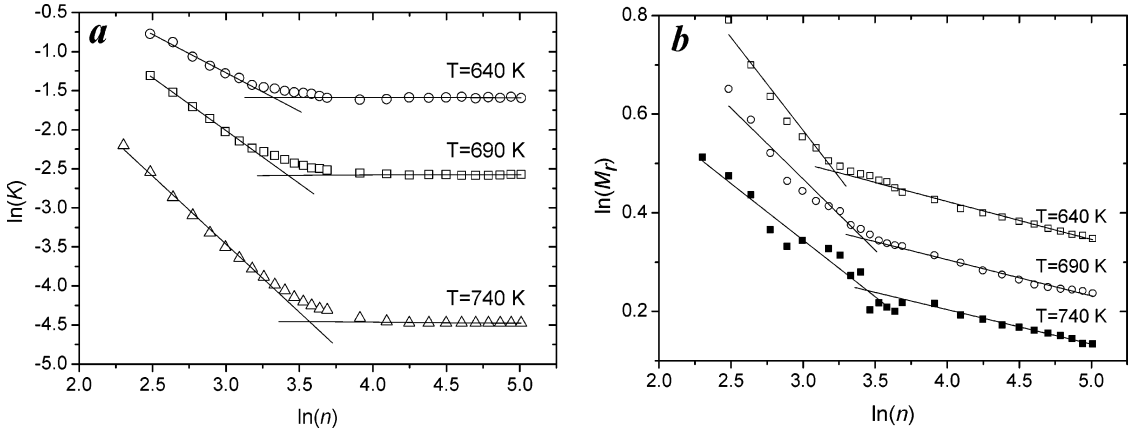

Figure 10. Same as Figure 7 but on a logarithmic scale. The symbols represent MD data obtained via eq 11, and the solid lines are fitted lines. The data for part b were shifted for clarity upward by 0.1 at 690 K and by 0.2 at 640 K.

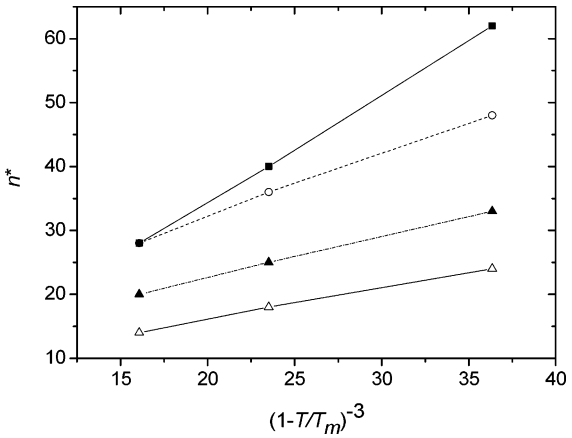

Figure 11. Temperature dependences of various estimated values, n^*: upper solid line, proposed extrapolation of ref 7; bottom solid line, n^* determined from MD steady state rate by the Zeldovich−Wu method; uppermost dashed line, bifurcation points of time lags; intermediate dot−dashed line, intersection points of logarithmic plots of nucleation rates and reduced moments.

Conclusions

An approach based on probability was adopted to solve the nucleation problem in the transient regime. In conventional methods of analysis of data, such an approach can be used only in the case of supercritical nuclei sizes. On the other hand, the method of times of first appearance avoids the overshooting of reduced flux and makes possible the Miloshev probabilistic interpretation for the subcritical region, as well. However, solutions are sensitive to the assumed probability distribution function. We used two such functions. The first function was taken from Wu.[10] His log-normal distribution gave unstable results for $n < n^*$ in the nucleation studied here. The second function was based on a modified Shneidman function for reduced flux. Although this function is significantly different from solutions of the Becker−Döring equations as $t \rightarrow 0$, it gave quite good results for all of our MD data.

We used cumulative probability functions with two adjustable parameters which were expressed through the zeroth and first moments. That affords an opportunity to discuss the kinetics of nucleation in the same language for the two different functions. The 0th moment is time lag commonly cited. The reduced moment defined in the foregoing is a parameter characterizing how rapidly or slowly the reduced flux goes from zero to unity. The third adjustable parameter is the steady state nucleation rate. It is independent of nuclear size in conventional analyses but depends on nuclear size in the method of times of first appearance adopted in this investigation.

The log-normal and our trial probability distribution functions give similar dependences of the nucleation parameters on nuclear size in many cases. We discussed in detail only those solutions based on our trial function, because it usually gave better and more stable results for our MD data than did the log-normal one, at least when nuclei were small.

There are two regions in the plots of derived parameters as a function of nuclear size. Curiously, time lags do not depend on temperature and increase linearly with n in the initial stages of nucleation. For nuclei above the critical size, however, the time lag varies logarithmically with the size of nuclei and, as might be expected, is higher, the larger the nucleus. Nucleation rates and reduced moments depend only weakly on n in the supercritical region, but they increase substantially as n decreases in the subcritical region. Values of the reduced moment depend slightly on temperature and are comparable in behavior to those found[4] for SeF_6. These similarities occur despite the very great differences in the forces binding the systems together. Salt is very eager to nucleate, exhibiting substantially larger rates at a given degree of supercooling than observed for the SeF_6 system.

The most novel aspect of the new method of times of first appearance is its ability to reveal the size of critical nuclei. Applying the criterion for n^* based on the Zeldovich solution of the Becker−Döring equations, we estimated the critical nucleus sizes to be 14, 18, and 24 ions for quench temperatures of 640, 690, and 740 K, respectively.

Acknowledgment. We thank Dr. D. T. Wu for helpful discussions.

References and Notes

(1) Djikaev, Y. S.; Tabazadeh, A.; Reiss, H. *J. Chem. Phys.* **2003**, *118*, 6572.
(2) Turnbull, D.; Fisher, J. C. *J. Chem. Phys.* **1949**, *17*, 71.
(3) Turnbull, D. *J. Chem. Phys.* **1952**, *20*, 411.
(4) Bartell, L. S.; Turner, G. W. *J. Phys. Chem. B* **2004**, *108*, 19742.
(5) Huang, J.; Zhu, X.; Bartell, L. S. *J. Phys. Chem. A* **1998**, *102*, 2708.
(6) Koishi, T.; Yasuoka, K.; Ebisuzaki, T. *J. Chem. Phys.* **2003**, *119*, 11298.
(7) Valeriani, C.; Sanz, E.; Frenkel, D. *J. Chem. Phys.* **2005**, *122*, 194501.
(8) Miloshev, N. *Atmos. Res.* **1992**, *28*, 173.
(9) Frisch, H. L. *J. Chem. Phys.* **1962**, *36*, 510.
(10) Wu, D. In *Solid State Physics*; Ehrenreich, H., Spaepen, F., Eds.; Academic Press: New York, 1997; Vol. 50, p 38.
(11) Becker, R.; Döring, W. *Ann. Phys.* **1935**, *24*, 719.
(12) Zeldovich, Ya. B. *Acta Physicochim. URSS* **1943**, *18*, 1.

(13) Abraham, F. F. *J. Chem. Phys.* **1969**, *51*, 1632.
(14) Kelton, K. F.; Greer, A. L.; Thompson, C. V. *J. Chem. Phys.* **1983**, *79*, 6261.
(15) Allen, M. P.; Tildesley, D. J. *Computer Simulations of Liquids*; Clarendon Press: Oxford, U.K., 1989.
(16) Tosi, M. P.; Fumi, F. G. *J. Phys. Chem. Solids* **1964**, *25*, 45.
(17) van Duijneveldt, J. S.; Frenkel, D. J. *Chem. Phys.* **1992**, *96*, 4655.
(18) ten Wolde, P. R.; Ruiz-Montero, M. J.; Frenkel, D. *J. Chem. Phys.* **1996**, *104*, 9932.
(19) Chushak, Y. G.; Bartell, L. S. *J. Phys. Chem. A* **2000**, *104*, 9328.
(20) Sevic, E. M.; Monson, P. A.; Ottino, J. M. *J. Chem. Phys.* **1988**, *88*, 1198.
(21) Tikhonov, A. N.; Arsenin, V. Y. *Solution of Ill-Posed Problems*; Winston, Wiley: New York, 1977.
(22) Nowakowski, B.; Ruckenstein, E. *J. Colloid Interface Sci.* **1991**, *145*, 182.
(23) Shneidman, V. A. *J. Chem. Phys.* **2001**, *115*, 8141.
(24) Shneidman, V. A. *J. Chem. Phys.* **2003**, *119*, 12487.
(25) Gumbel, E. J. *Statistics of Extremes*; Columbia University Press: New York, 1958.